Chapter 18
Morphological Features of Nanostructured Sensor for X-Ray and Optical Imaging, Based on Nonideal Heterojunction

Ie. Brytavskyi, V. Smyntyna, and V. Borschak

Abstract A novel nanostructured sensor for X-ray and optical images obtaining is developed on the basis of nonideal heterojunction CdS-Cu_2S. Microscopy studies have been conducted to determine the optimum method of sensor manufacturing. The analysis of the original data set with microscopic image comparison of polycrystalline films on different technological parameters showed that the most homogeneous surface structure presents on samples, which CdS layer is obtained by vacuum thermal evaporation of CdS layer. This finding is consistent with results of current-voltage characteristics analysis, which showed the presence of high quality CdS-Cu_2S heterostructure, obtained by mentioned base layer forming methodics.

18.1 Introduction

The polycrystalline films containing Cu_2S-CdS heterostructure formed by dry deposition method [1] have been investigated in this work. The heterostructures were formed by employing a substitution technique where the nanolayer of copper sulfide is formed directly on the substrate layer of CdS during heat treatment using a pre-printed cuprous chloride film, formed by vacuum evaporation. This technology is promising due to low cost, easy processibility, and the possibility to fabricate large area films with satisfactory structural quality [2].

However, such a heterojunction consisting of *p*-type Cu_2S and *n*-type CdS is a rather complicated structure because of the interface between two materials with different electron affinities, band gaps, and polycrystalline structures. The lattice mismatch and interdiffusion of components might cause defects at or near the interface that strongly affect the junction properties [3].

Sensor based on nonideal heterojunction CdS-Cu_2S demonstrates the properties of internal amplification and signal accumulation effect [3–5], and substantially

Ie. Brytavskyi (✉) • V. Smyntyna • V. Borschak
Odessa I.I. Mechnikov National University, Dvorianska str. 2, 65028 Odessa, Ukraine
e-mail: brytav@ukr.net

© Springer Science+Business Media Dordrecht 2016

J. Bonča, S. Kruchinin (eds.), *Nanomaterials for Security*, NATO Science for Peace and Security Series A: Chemistry and Biology, DOI 10.1007/978-94-017-7593-9_18

increased sensitivity compared to existing analogues. Practically valuable results towards the measuring devices and systems creation for using on new telecommunication and testing methods were obtained.

Actuality of designed sensor implementing is defined by opportunity of creation on its basis a large sensing area devices that can be used in various security systems. Developed sensor has outstanding practical importance because it can be used for creation new classes of nanostructured sensors based on nonideal heterojunction which are the part of functional nanoelectronics devices.

18.1.1 Sensor Samples Obtaining

A transparent SnO_2 layer with 200 nm thickness was deposited on a glass substrate in vacuum to serve as the back electrode. The CdS layer was then deposited by one of two used methodics: vacuum thermal evaporation [6] (VTE) of pure CdS powder at the rate of $\sim$0.3 μm/min at 200 °C or electrohydrodynamical spraying [7] (EHDS) at room temperature under applied voltage about 35 kV. The evaporation time was varied from 60 to 80 min to get a CdS layer thick enough (15–26 μm) and to prevent shunting due to diffusion of copper ions, as a Cu_2S layer is subsequently formed on the top of the CdS layer. Thickness increase of the CdS layer results in an unacceptable increase of the base region resistivity. Thickness of 20–24 μm was found to be optimal for the CdS base layer. Spraying time varied in range 3–10 min to get a continuous layer of CdS with thickness up to 5 μm.

The top layer and heterostructure were formed by a substitution reaction technique [1] where a layer of copper sulfide is formed by reacting the base CdS layer [3] with a subsequently deposited layer of CuCl. The samples with CuCl film on the surface were heated at 200 °C for 4 min in a vacuum chamber to initiate and maintain a solid-phase substitution reaction (18.1).

$$CdS + 2CuCl \rightarrow Cu_2S + CdCl_2. \tag{18.1}$$

Thickness of the Cu_2S layer was controlled by varying the CuCl deposition time. The metallic top electrode was made by evaporation technique or using pressed needle-type contact to the surface of Cu_2S layer.

18.2 Microscopic Study of CdS-Cu_2S Heterostructure Film Layers

Investigation of surface morphology of photosensitive thin film samples were carried out using two instruments: atomic force microscope (AFM) NTEGRA Prima NS-150 using a silicon cantilever with a 10 nm radius tip of the probe and a scanning electron microscope (SEM) Inspect F50 with a maximum resolution of 1.0 nm at 30 kV operating potential on the cathode.

18.2.1 Atomic Force Microscopy

Scanning of sensor samples surface occurred in static contact mode, image processing and statistical analysis were performed using Nova 1138 and Gwyddion software. The main goal here was to compare changes in the characteristics of the surface morphology of investigated CdS-Cu_2S thin film structures in the manufacturing process, including observation and analysis of changes in the structural characteristics of the sample surface during the formation of the layer Cu_2S on CdS film.

Comparing the morphology of samples prepared by different technologies, using methods of atomic force microscopy, was impossible due to the peculiarities of surface structure of CdS base layer films, manufactured by electrohydrodynamic spraying. When trying to scan these samples, the probe signal almost immediately underwent to irreversible distortions. Further use of the probe turned out to be impossible. In the study by electron microscope it was established the presence of CdS microparticles, that were adhering to the probe tip and made impossible its further operation.

For samples obtained by vacuum thermal evaporation, scanning was performed successfully and typical distributions of surface morphology presented on Fig. 18.1.

Used AFM technique allowed the quantitative analysis of morphology on a number of parameters such as roughness R_a (a set of surface irregularities with small steps at the base length), waviness W_a (a set of repetitive irregularities in which the distance between adjacent elevations or valleys exceeds the basic length), the relative length of the profile L_r (the ratio of the length of the profile to the basic length) and average grain size.

This enabled the comparison of thin film sample surface microgeometry before and immediately after the formation of Cu_2S layer on CdS. Thus, for the same

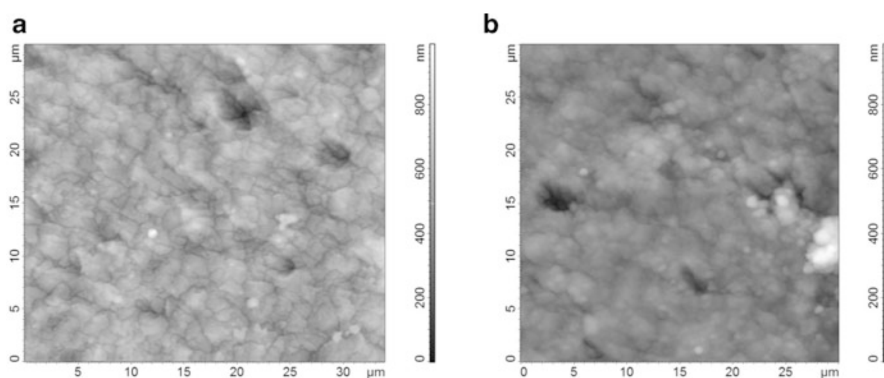

Fig. 18.1 AFM image of the sample surface before and after the heterojunction formation. (**a**) – the surface of CdS film, obtained by VTE, (**b**) – the surface Cu_2S layer, formed on the CdS. Scans are in the same scale

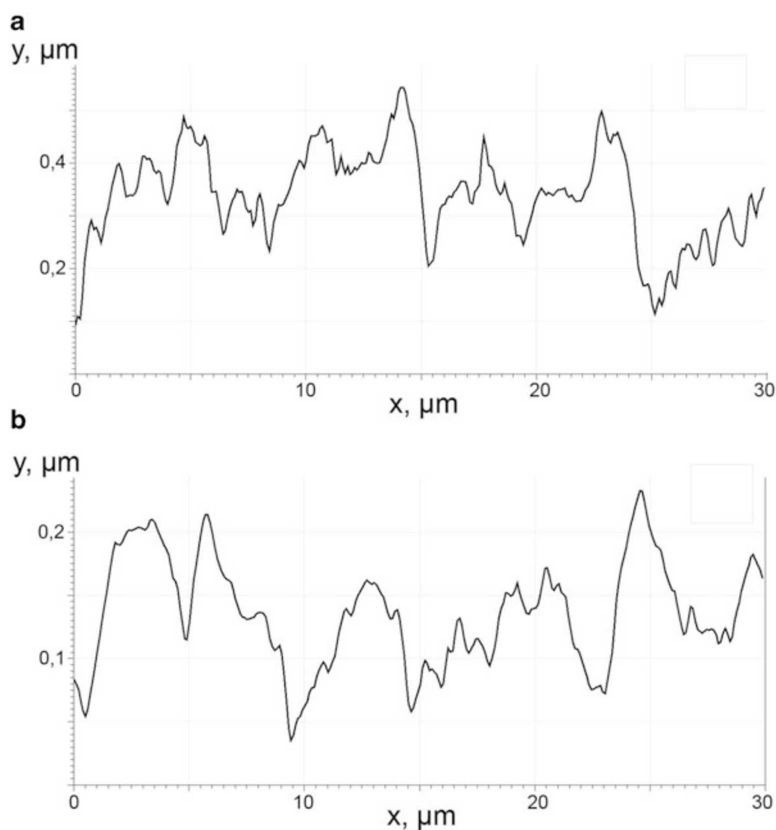

Fig. 18.2 Linear profiles of the surface for the base CdS layer, obtained by VTE (**a**) and for Cu_2S layer, formed on the surface of the same sample (**b**)

Table 18.1 The morphological parameters of the surface of CdS and Cu_2S layers

Parameter	CdS	Cu_2S
Average roughness R_a, μm	0.050	0.027
Average waviness W_a, μm	0.364	0.193
Relative length of profile L_r, a.u.	1.018	1.003

sample the sets of linear surface profiles for CdS layer and then for later deposited Cu_2S layer were obtained. Typical morphological profiles of the samples are shown on Fig. 18.2 (a – CdS, b – Cu_2S).

The values of morphological parameters numerically obtained from the profiles are presented in Table 18.1. It is seen that formation layer reduces the expression of Cu_2S surface microrelief, thereby the values of roughness and waviness decrease. The relative length L_r of the profile also reduced. Considering that the actual surface area is L_r^2 times more, then geometric one, so the deposition of Cu_2S layer reduces the effective area of the sample in the L_r^2 (CdS) – L_r^2 (Cu_2S) = 0.003, i.e. 3 %.

18.2.2 *Scanning Electron Microscopy*

The using of scanning electron microscopy allowed making the qualitative and quantitative comparative analysis of the surface microstructure for both types of samples, obtained by different base layer forming technologies.

The images of surface of sensor elements obtained using methods EHDS and VTE are shown in the same scale on the Fig. 18.3. The comparing of the surface images for CdS (Figs. 18.3a, c) clearly shows that there is more textured surface for EHDS samples, the granular structure of the base material is clearly seen. It was found that the CdS film, obtained by EHDS have a polycrystalline structure, orientation of polycrystallines is chaotic, average size of crystallites in the

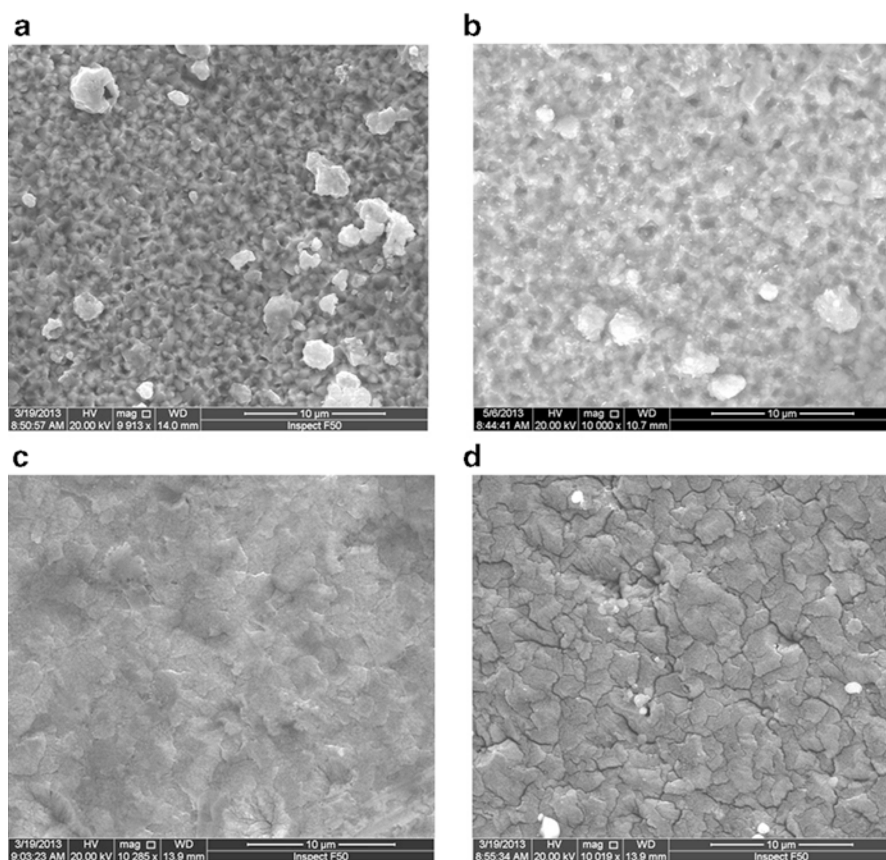

Fig. 18.3 SEM image of the sample before and after heterojunction formation. (**a**) – the surface of CdS film, obtained by EHDS method, (**b**) – the surface of Cu_2S layer, formed on the EHDS CdS, (**c**) – the surface of CdS film, obtained by VTE method, (**d**) – the surface of Cu_2S layer, formed on the VTE CdS. Zomming rate – $10{,}000^x$

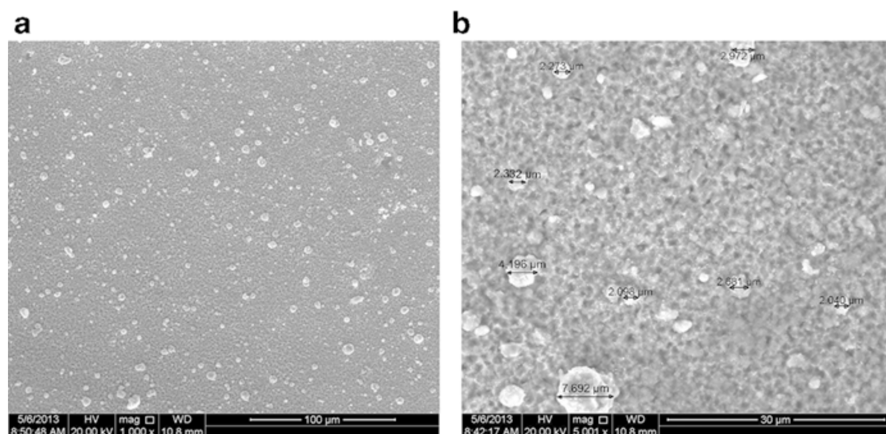

Fig. 18.4 SEM image of CdS film surface, obtained by EHDS method: (**a**) – 1000^x zoom (**b**) – 5000^x zoom. Measured linear dimensions of observed microparticles are marked

measurements on the SEM scan was 0.8 μm. The surface of VTE samples shows opposite – the relative homogeneity and less expressed relief.

Repeated scan series of sensor samples were made after forming the copper sulfide film on CdS layer by a substitution reaction in the solid phase. Both types of heterojunction samples, EHDS (Fig. 18.3b) and VTE (Fig. 18.3d) were investigated. This made it possible to compare the morphology of the surface as before and after the formation of the upper layer Cu_2S, and as between technological types of samples.

The splitting of Cu_2S layer surface to separate flakes about 5 μm^2 was observed for VTE samples (Fig. 18.3d) such features were not observed on the surface of EHDS samples (Fig. 18.3b).

SEM studies revealed the presence of particles on the surface that prevent the use of AFM techniques for scanning EHDS samples (Fig. 18.4a). The size of these particles ranged from 1 to 8 μm (Fig. 18.4b). They can easily separate from the surface of CdS by passing of AFM probe tip and stick on it, and that process make it impossible to use atomic force microscopy techniques for this type of samples. The formation of these particles is likely due to the presence of very large drops in the spray flare. When passing the reaction (18.1) the crystalline conglomerates on the substrate are formed of these droplets, and they are observed in SEM images as close to spherical shape particles on the surface of the sample.

A separate important task using microscopic methods was to study not only the surface but also the bulk characteristics of CdS-Cu_2S sensor heterostructures. For this part of the samples was taken away from the set to the cleavage procedure: cutting of the glass substrate and subsequent breakage by the incision line. In the majority of cases obtained cut was strictly perpendicular to the plane of the substrate glass plate on the side, where the heterojunction layers were deposited.

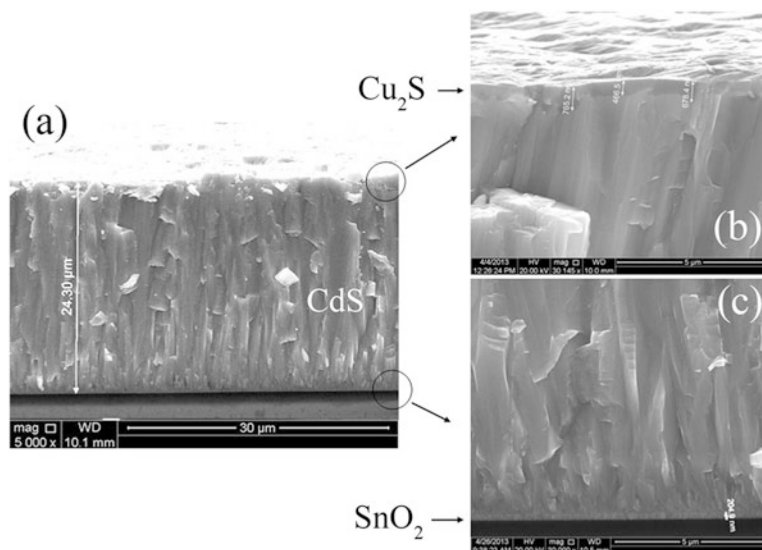

Fig. 18.5 SEM image of thin film heterojunction cross-section: general view at 5000^x zoom (**a**), the surface region with Cu_2S layer (**b**) and contact area with SnO_2 layer on a glass substrate (**c**) at $30{,}000^x$ zoom

The control of perpendicular matching of the cut line of the surface was held in electron microscope camera using a mobile holder, which allowed to make sample scanning from any side.

General view of CdS-Cu_2S nanoheterostructure cross-section with the base layer obtained by VTE is shown on Fig. 18.5. For this type of samples the columnar structure of crystals location in cadmium sulfide was revealed, which is consistent with the model of diffusion of copper to base layer by deep intercrystalline layers [1].

The precise measurements of geometric parameters of sensor samples, such as the thickness of the layers of the heterostructure, were obtained. The equipment allowed to carry out measurements directly on the sample in the scan mode. Zooming up to 30,000 times made it possible to distinguish tin oxide contact layer (Fig 18.5c). The thickness of SnO_2 for all samples was identical and uniform within 200 ± 20 nm (Fig. 18.6). Thickness of base layers CdS obtained by VTE method was in range 15–25 µm (Fig. 18.5a) for EHDS method – 1–4 µm (Fig. 18.4b). These data correspond well to the results of previous indirect measurements [8] of the thickness of the base layer (interferometry, chemical etching, film transparency measuring), but unlike them, method used in this work is a source of direct and most accurate values of the thickness of the layers CdS and Cu_2S (actual accuracy to 3 nm is limited by resolution of the device).

SEM cross-section image of EHDS base layer is presented on Fig. 18.7. CdS layer thickness is about 3 µm. However, in this case, the columnar structure of

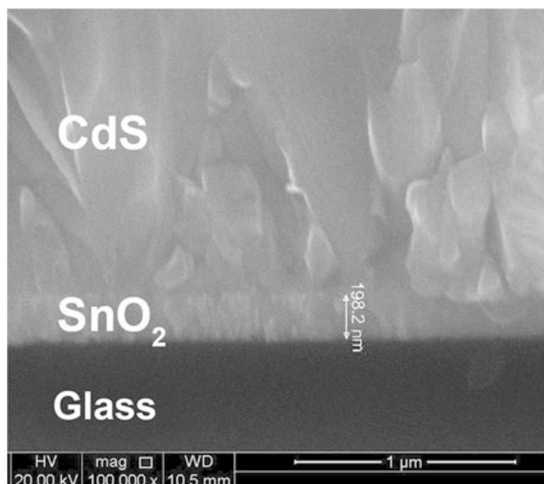

Fig. 18.6 SEM image of contact area cut with CdS base layer on glass substrate at 100,000^x zoom. The *arrow* indicates the measured thickness of SnO_2 contact layer

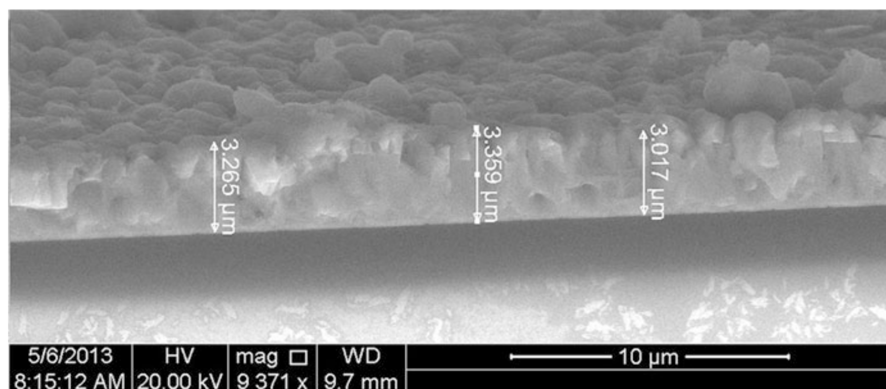

Fig. 18.7 SEM image of cross-section of sample formed by EHDS technology at 5000^x zoom

crystallites was not observed. Instead, visible grains location disorder, significant surface roughness and thickness variation comparable to the value of layer thickness were evident.

According to obtained linear measurements the characteristic curve of layer thickness dependence on film deposition time for VTE technology was built (Fig. 18.8). The difference between previously obtained and a new curve is due to insufficient precision of previous indirect measurement techniques [8] (electrochemical etching and CdS film optical transparency). A new curve shows also previously unmarked shift from linear dependence h (t_{dep}) to sublinear for larger time values. Thus, a decrease in growth rate of the film over time in the later stages of the CdS layer forming is observed, which can be explained by a decrease in the intensity of source material evaporation in a vacuum chamber.

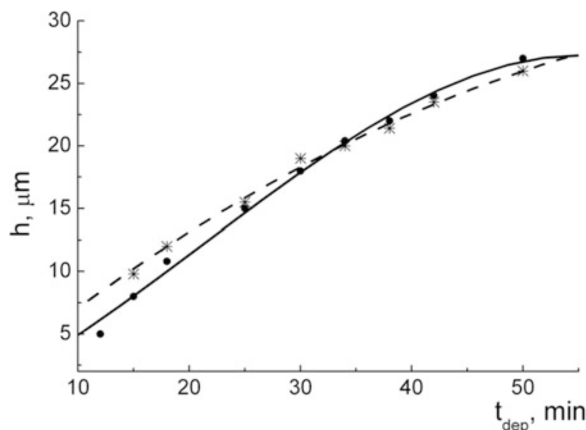

Fig. 18.8 The dependence of thickness (h) of CdS film on time (t_{dep}) of its deposition by VTE method. Thickness values calculated from experimental measurements of transparency coefficient (*stars*, *dotted line*) and measured directly on the SEM image of sectioned sample (*circles*, *solid line*)

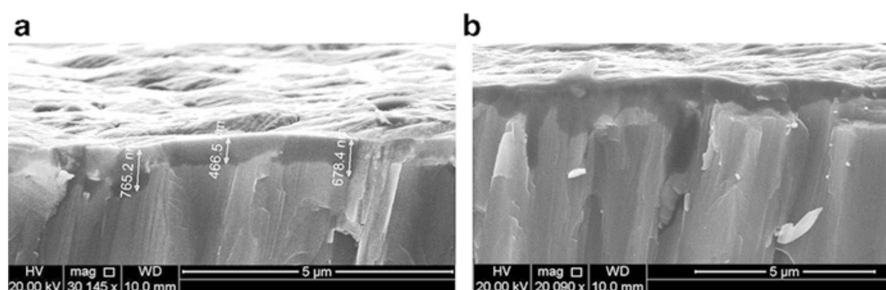

Fig. 18.9 SEM image of heteojunction surface area cross-section with 30,000^x zooming (**a**) and with 20,000^x zooming (**b**). The *arrows* indicate measured thickness of Cu_2S layer

The big difference between the values of conductivity of layers CdS and Cu_2S, and therefore between the intensity of electron scattering of scanning beam, allowed to observe copper sulfide layer directly formed by substitution reaction on the surface of CdS (Fig. 18.5b). Thus, the opportunity was used to receive the original results for investigated structures concerning the distribution of thickness h_1 of the light-absorbing upper layer Cu_2S. Thus, a detailed scan revealed a significant heterogeneity in thickness of copper sulfide film, as shown in Fig. 18.9. Measured range in thickness was 0.3–2 μm with an average 0.75 μm. Considering that most of the long-wavelength light is absorbed by a copper sulfide film, we can speak about significant local inhomogeneities in the intensity of light absorption in Cu_2S caused by varying of layer thickness.

Additional scanning of CdS layer cross-section revealed the presence of surface cracks with depth h_2 up to 1.5 μm (Fig. 18.10). These cracks can play the role of effective channels for Cu_2S layer thickening with subsequent diffusion of copper atoms deep into CdS film. Filling the cracks by copper sulfide, that is formed during the substitution reaction, changes the sensor surface roughness that was observed during the study of samples microrelief by AFM. Typical local increase in Cu_2S

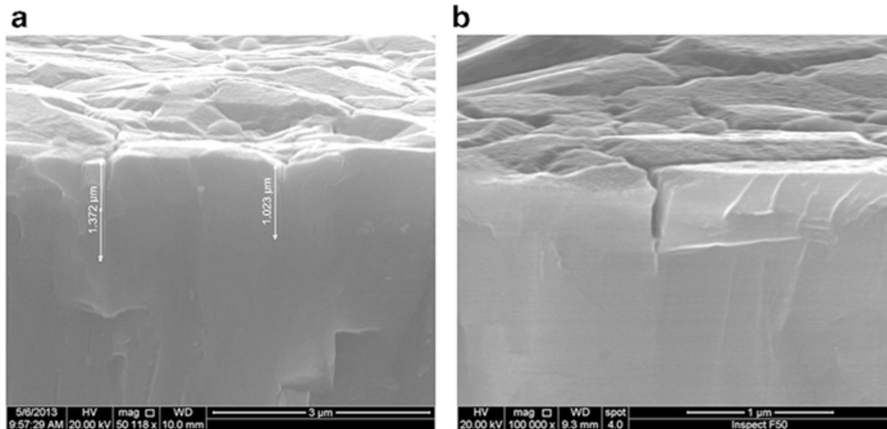

Fig. 18.10 SEM image the surface area cross-section of the base layer CdS, obtained by VTE, with 50,000^x (**a**) and 100,000^x (**b**) zooming. The *arrows* indicate measured depth of detected intercrystalline cracks

thickness was in rage of 1.5–2 μm (Fig. 18.10b), which is completely consistent with the possibility of its formation due to surface cracks in CdS.

Thus, in the use of VTE method of CdS base layer obtaining with subsequent substitution reaction to create a surface Cu_2S layer a "vertical" heterojunction is formed, when copper sulfide layer gets deeper in the base region due to the presence of surface cracks. This increases the heterojunction effective area and therefore leads to increasing of short circuit current and efficiency of photoconversion sensor.

According to obtained SEM microscopy results the model of surface microstructure of studied heterostructure was developed ant its visualization is given on Fig. 18.11, which shows an expected technological thickness $h_1$of Cu_2S layer and thickness irregularities caused by cracks in the surface layer of CdS with depth h_2.

The presence of cracks with 2 μm depth in the surface layer of cadmium sulfide formed by vacuum thermal evaporation was revealed. It was proved that these intercrystalline cracks promote the penetration of Cu_2S compound into base layer depth when forming heterojunction, as it was evidenced by local heterogeneity of measured Cu_2S thickness. This fact can explain observed variations in sensor surface photosensitivity [9].

18.3 Conclusion

Novel results concerning CdS-Cu_2S heterojunction surface morphology and layers geometrical distribution were obtained. In particular, the question of observed variation of surface photosensitivity caused by irregularities in thickness of light-absorbing Cu_2S layer were clarified. Also the comparison of samples formed

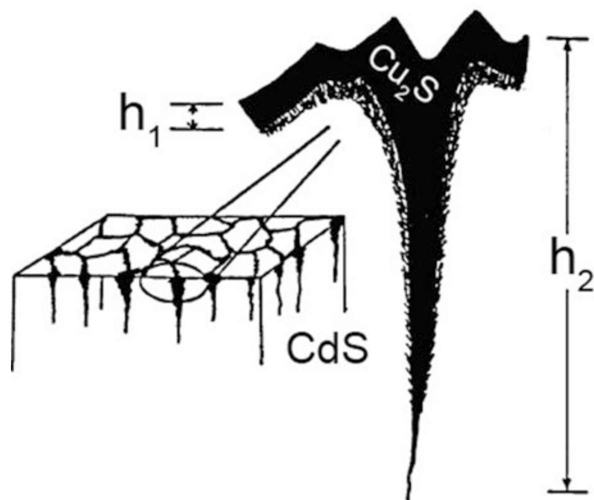

Fig. 18.11 Illustration of CdS-Cu_2S sensor heterostructure surface morphology according to performed SEM research, h_1 – thickness of Cu_2S; h_2 – depth of cracks in CdS surface layer

by two different methodics (electrodynamical spraying and vacuum evaporation techniques) was made. Obtained results enable to understand better the features of layers forming procedure, the junction components surface interaction and influence of external environment on sensor samples surface characteristics.

Reliable characteristic dependence of CdS thickness on evaporation time was also obtained, which enables more accurate process of films geometric parameters control during the formation of heterojunction layers and enables the doping of individual layers of the base layer by introducing an impurity substance at a certain time of CdS film depositing.

Developed sensor prototype demonstrates high stability parameters and shows prospectivity for comprehensive studies of inorganic, organic and biological objects. The originality of designed nanostructured sensors consists in the fact that they are effective at low doses of X-ray radiation, which makes it possible to use this material not only in controlling production processes, but in places of public use, such as security systems and customs control.

References

1. Goldenblum A, Oprea A (1994) Photocapacitance effects in dry processed Cu_2S-CdS heterojunctions. J Phys D 27:582–586
2. Vanhoecke E, Burgelman M, Anaf L (1986) Reactive sputtering of large-area Cu_2S/CdS solar cells. Thin Solid Films 144:223–228
3. Borschak VA, Brytavskyi Ie V, Smyntyna VA, Lepikh Ya I, Balaban AP, Zatovskaya NP (2012) Influence of internal parameters on the signal value in optical sensor based on the non-ideal heterostructure CdS-Cu_2S. Semicond Phys Quantum Electron Optoelectron 15(1):41–43

4. Borschak VA, Smyntyna VA, Brytavskyi Ie V, Karpenko AA, Zatovskaya NP (2013) Open-circuit voltage of an illuminated nonideal heterojunction. Semiconductors 47(6):838–843
5. Gaubas E, Borschak V, Brytavskyi I, Ceponis T, Dobrovolskas D, Jursenas S, Kusakovskij J, Smyntyna V, Tamulaitis G, Tekorius A (2013) Non-radiative and radiative recombination in CdS polycrystalline structures. Adv Condens Matter Phys 2013:1–15
6. Goldenblum A, Popovici G, Elena E, Oprea A, Nae C (1986) All-evaporation-processed Cu_2S/CdS solar cells with improved characteristics. Thin Solid Films 141:215–221
7. Nascu C, Pop I, Ionescu V, Indrea E, Bratu I (1997) Spray pyrolysis deposition of CuS thin films. Mater Lett 32(2):73–77
8. Vassilevski DL (1999) Physical principles of graphic registration by non-ideal heterojunction. Sens Actuators A 55:167–172
9. Borschak VA, Smyntyna VA, Brytavskyi Ie V, Balaban AP, Zatovskaya NP (2011) Dependence of conductivity of an illuminated nonideal heterojunction on external bias. Semiconductors 45(7):894–899